• Basic Research •

Silencing SLC31A1 attenuates high glucose plus copper-induced cuproptosis-like signaling, oxidative stress, and barrier dysfunction in human retinal microvascular endothelial cells

Ying Li[1], *Meng Chen*[2], *Han-Guang Dong*[3]

[1]Shanghai Eye Diseases Prevention & Treatment Center/ Shanghai Eye Hospital, School of Medicine, Tongji University, Shanghai 200336, China
[2]Department of Opthalmology, Qingdao Municipal Hospital, Qingdao 266011, Shandong Province, China
[3]Department of General Surgery, Shanghai General Hospital, Shanghai Jiao Tong University School of Medicine, Shanghai 200080, China
Correspondence to: Han-Guang Dong. Department of General Surgery, Shanghai General Hospital, Shanghai Jiao Tong University School of Medicine, Shanghai 200080, China. dhg755@163.com
Received: 2025-12-03 Accepted: 2026-04-22

Abstract

● **AIM:** To examine whether SLC31A1 knockdown protects human retinal microvascular endothelial cells (HRMECs) exposed to high glucose and copper.

● **METHODS:** HRMECs were exposed to normal glucose (5 mmol/L) or high glucose (30 mmol/L), with or without 50 μmol/L $CuSO_4$ during the final 6h, and transfected with control or SLC31A1 small interfering RNA. Cell viability (cell counting kit-8) and adenosine triphosphate (ATP) content were measured. Oxidative stress was assessed by glutathione/oxidized glutathione ratio, malondialdehyde, superoxide dismutase, catalase, and reactive oxygen species. Intracellular copper and mRNA levels of SLC31A1, ferredoxin 1, lipoic acid synthetase, dihydrolipoamide S-acetyltransferase (DLAT), and tight junction genes were quantified. SLC31A1 protein and lipoylated DLAT were detected by Western blotting. Endothelial barrier function was evaluated by fluorescein isothiocyanate-dextran permeability and transendothelial electrical resistance.

● **RESULTS:** High glucose alone caused modest loss of viability, ATP depletion, increased oxidative stress, downregulation of tight junction genes, and mild barrier impairment, with minimal additional effect of SLC31A1 knockdown. Copper supplementation under high glucose induced marked intracellular copper overload, enhanced DLAT lipoylation, severe ATP loss, oxidative injury, and pronounced barrier dysfunction. SLC31A1 knockdown significantly reduced copper accumulation, lipoylation of DLAT, and oxidative stress, preserved ATP and viability, and partially restored tight junction gene expression and barrier function, although none of these parameters returned to normal glucose levels.

● **CONCLUSION:** SLC31A1-dependent copper influx appears to contribute to cuproptosis-associated mitochondrial energy failure, oxidative stress, and barrier breakdown in high glucose-exposed retinal endothelial cells, indicating that SLC31A1 may represent a potential therapeutic target for diabetic retinal microvascular protection.

● **KEYWORDS:** SLC31A1; cuproptosis-like signaling; diabetic retinopathy; retinal microvascular endothelial cells; oxidative stress

DOI:10.18240/ijo.2026.08.04

Citation: Li Y, Chen M, Dong HG. Silencing SLC31A1 attenuates high glucose plus copper-induced cuproptosis-like signaling, oxidative stress, and barrier dysfunction in human retinal microvascular endothelial cells. *Int J Ophthalmol* 2026;19(8):1461-1469

INTRODUCTION

Diabetic microvascular disease (DMiVD), encompassing diabetic kidney disease, diabetic retinopathy (DR), and distal symmetrical polyneuropathy, is a major global cause of end-stage renal disease, blindness, limb amputation, and foot ulcers, with DR being one of the most common complications and a leading cause of visual impairment across all age groups[1]. In 2020, an estimated 103 million people were living with DR, and this number is projected to increase to 161 million by 2045[2]. DR is now recognized as the only cause of blindness whose prevalence has continued to rise between 1990 and 2020, especially in adults over 50 years of age[3]. Anti-vascular endothelial growth factor (anti-VEGF) therapy is currently the mainstay treatment for vision-threatening stages

of DR[4], yet repeated intraocular injections, high cost, and incomplete or transient responses in a substantial proportion of patients underscore the need for new mechanisms and targets to more effectively prevent and treat diabetic retinal microvascular injury.

Copper (Cu) is an essential trace element that cycles between Cu^{2+} and Cu^{+} and serves as a cofactor for enzymes involved in redox balance, electron transfer, and metabolism[5]. However, Cu dyshomeostasis can promote reactive oxygen species (ROS) generation and cellular injury. Emerging clinical and experimental evidence links altered Cu metabolism to diabetes and its complications, including DR[6-8]. In parallel, the newly described regulated cell death pathway cuproptosis has connected mitochondrial Cu overload with protein lipoylation, bioenergetic failure, and cell death[9]. SLC31A1 (also known as CTR1) is the major high-affinity Cu importer in mammalian cells, whereas copper-transporting P-type ATPases (ATP7A and ATP7B) regulate Cu efflux and intracellular redistribution[5]. In endothelial cells, SLC31A1 also functions as a redox-sensitive regulator of vascular endothelial growth factor receptor 2 (VEGFR2) trafficking and angiogenic signaling[10]. Recent DR-related studies further identified SLC31A1 as a cuproptosis-related hub associated with retinal inflammation and immune-cell infiltration[7]. Together, these findings suggest that dysregulated SLC31A1-dependent Cu handling may intersect with oxidative stress, inflammatory activation, and vascular dysfunction in the diabetic retina.

Despite these advances, whether SLC31A1 directly mediates Cu-dependent injury in human retinal microvascular endothelial cells (HRMECs) remains unknown. This represents an important gap because HRMECs are core structural and functional components of the inner blood-retinal barrier, and endothelial dysfunction is an early event in DR. Moreover, most previous DR studies assessed whole retinal tissue or microglia rather than dissecting endothelial mechanisms *in vitro*. Recent work has further supported the vulnerability of retinal endothelial cells to hyperglycemic stress, showing that 30 mmol/L high glucose directly alters the viability, migration, tube formation, and VEGF/PI3K signaling of human retinal endothelial cells[11]. Therefore, we used siRNA-mediated SLC31A1 knockdown in HRMECs exposed to high glucose with or without Cu overload to evaluate cell viability and adenosine triphosphate (ATP) content, oxidative stress, intracellular Cu accumulation, cuproptosis-related signaling, and barrier function. We hypothesized that limiting SLC31A1-mediated Cu influx would attenuate Cu-aggravated endothelial injury under diabetic-like conditions.

MATERIALS AND METHODS

Ethics Statement This study used commercially obtained HRMECs and did not involve human participants, identifiable human samples, or animal experiments. Therefore, approval from an ethics committee or institutional review board was not required.

Cell Culture Primary HRMEC (ACBRI-181, Cell Systems, Kirkland, WA, USA) were used. For recovery, vials were thawed in a 37℃ water bath for <1min, surface-disinfected, transferred into pre-warmed complete growth medium, and centrifuged (600 g, 4℃, 5–10min). The pellet was briefly resuspended with 200 μL CultureBoost™ (Cell Systems, Kirkland, WA, USA) and then gently diluted with 37℃ medium before seeding. Culture vessels were pre-coated with Attachment Factor™ (Cell Systems, Kirkland, WA, USA) according to the manufacturer's instructions. Cells were maintained at 37℃, 5% CO_2, and 95% relative humidity in Cell Systems Complete Classic Medium (4Z0-500, Cell Systems, Kirkland, WA, USA) supplemented as recommended. The first medium change was performed 12h after thawing, and every 48h thereafter. Cells at low passage (P6) were used for all experiments.

Cell Grouping HRMECs were allocated to normal glucose (NG; 5 mmol/L D-glucose, 48h), high glucose (HG; 30 mmol/L D-glucose, 48h[11]), HG+control small interfering RNA (siCtrl), HG+SLC31A1 small interfering RNA (siSLC31A1), HG+Cu+siCtrl, and HG+Cu+siSLC31A1. In the Cu-overload groups, 50 μmol/L $CuSO_4$ was added during the final 6h of HG exposure. This condition was selected as a literature-informed acute Cu challenge based on prior endothelial-cell studies using Cu in the 25–100 μmol/L range, as well as retinal-cell literature reporting high glucose combined with approximately 50 μmol/L Cu in human retinal pigment epithelial cell line adult retinal pigment epithelial-19 (ARPE-19)[12-13]. Reagent stocks were prepared as follows: $CuSO_4 \cdot 5H_2O$ (catalog no. 939315, Merck KGaA, Darmstadt, Germany), 100 mmol/L in sterile water, and D-glucose (catalog no. G8644, Sigma-Aldrich, Merck KGaA, Darmstadt, Germany), 1 mol/L in sterile water. For siRNA transfection, cells were seeded in 6-well plates at 2×10^5 cells per well in serum-containing, antibiotic-free medium. At 60%–80% confluence, 50 pmol siRNA with 6 μL Santa Cruz Transfection Reagent (Santa Cruz Biotechnology, Dallas, TX, USA) in 1.0 mL transfection medium was applied for 6h, followed by addition of 1.0 mL twofold growth medium for 24h and then fresh complete medium. Cells were then switched to NG or HG, which was defined as time 0h. For Cu-overload conditions, 50 μmol/L $CuSO_4$ was added during the final 6h of HG exposure. Oxidative stress readouts, ATP levels, intracellular Cu, mRNA and protein expression, and permeability assays were performed at 72h after initiation of NG/HG exposure, with or without Cu.

Cell Counting Kit-8 Assays HRMECs were seeded in 96-well plates at 5×10^3 cells/well. Cell viability was assessed at 0, 24, 48, 72, and 96h after the start of NG/HG/HG+Cu exposure. At each time point, 10 μL of cell counting kit-8 (CCK-8) reagent was added directly to each well and incubated for 2h at 37°C. Absorbance at 450 nm was recorded using a microplate reader.

ATP, Oxidative Stress, and Intracellular Cu Assays Intracellular ATP levels were measured using a luciferase-based ATP assay kit (S0026, Beyotime Biotechnology, Shanghai, China) according to the manufacturer's instructions and expressed as a percentage of the NG group. Oxidative stress was evaluated with commercial kits from Beyotime Biotechnology (Shanghai, China) for reduced glutathione/oxidized glutathione (GSH/GSSG) ratio (S0053, A412), malondialdehyde (MDA; S0131S, A532; nmol/mg protein), total superoxide dismutase (SOD; S0101S, A450; U/mg protein), catalase (CAT; S0051, A520; U/mg protein), and intracellular ROS [S0034; 2',7'-dichlorodihydrofluorescein diacetate (DCFH-DA) fluorescence expressed as a percentage of the NG group)]. Intracellular Cu was quantified using a colorimetric Copper Assay Kit (MAK127, Merck KGaA, Darmstadt, Germany) following the manufacturer's protocol, and values were normalized to protein content (ng Cu per mg protein) determined by bicinchoninic acid (BCA) assay.

Quantitative Real-Time PCR Total RNA was extracted from HRMECs using TRIzol reagent (Invitrogen, Thermo Fisher Scientific, Waltham, MA, USA) and reverse-transcribed into cDNA with a commercial reverse transcription kit. Quantitative polymerase chain reaction (PCR) was performed using SYBR Green chemistry on a real-time PCR system (Thermo Fisher Scientific, Waltham, MA, USA). Relative mRNA expression was calculated using the $2^{-\Delta\Delta Ct}$ method with glyceraldehyde-3-phosphate dehydrogenase (GAPDH) as the internal control.

Western Blotting HRMECs were lysed in radioimmunoprecipitation assay (RIPA) buffer containing protease inhibitors, and protein concentrations were determined by BCA assay. Equal amounts of protein (30 μg per lane) were separated by sodium dodecyl sulfate-polyacrylamide gel electrophoresis (SDS-PAGE) and transferred onto polyvinylidene fluoride (PVDF) membranes. After blocking with 5% non-fat milk, membranes were incubated overnight at 4°C with primary antibodies against SLC31A1 (ab317432, Abcam, Cambridge, UK; 1:1000), total dihydrolipoamide S-acetyltransferase (DLAT, ab110332, Abcam; 0.5 μg/mL), lipoylated DLAT (lipo-DLAT, ab58724, Abcam, Cambridge, UK; 1:1000), and GAPDH (ab8245, Abcam, Cambridge, UK; 1:1000). Membranes were then incubated with the appropriate horseradish peroxidase (HRP)-conjugated secondary antibodies, including goat anti-rabbit immunoglobulin G (IgG) for SLC31A1 and lipoic acid-modified proteins, and goat anti-mouse IgG for total DLAT and GAPDH. Lipoylated DLAT was quantified at the DLAT-corresponding band. Bands were visualized using enhanced chemiluminescence and quantified by densitometry (ImageJ, National Institutes of Health, Bethesda, MD, USA). Protein levels were normalized to GAPDH, and the lipo-DLAT/total DLAT ratio was used as a readout of cuproptosis-related protein changes.

Paracellular Permeability Assay and Transendothelial Electrical Resistance HRMEC monolayers were established on 0.4-μm pore Transwell inserts and, after reaching confluence, were subjected to the indicated treatments for 72h before permeability assays. Fluorescein isothiocyanate (FITC)-dextran (70 kDa; ST2947, Beyotime Biotechnology, Shanghai, China) was diluted in serum-free medium to 1 mg/mL and added to the apical (upper) chamber at equal volumes per well, while the basolateral (lower) chamber contained an equal volume of serum-free medium. After incubation at 37°C with 5% CO_2 for 60min, medium from the lower chamber was collected and fluorescence was measured using a microplate reader (excitation 492 nm, emission 520 nm). Paracellular permeability was expressed as relative permeability normalized to the NG group. Transendothelial electrical resistance (TEER) was recorded using an epithelial volt-ohmmeter with chopstick electrodes (World Precision Instruments, Sarasota, FL, USA) according to the manufacturer's instructions. Inserts containing culture medium without cells served as blanks. TEER ($\Omega\cdot cm^2$) was calculated as (R_sample−R_blank)×membrane area and expressed as a percentage of the NG group.

Statistical Analysis All data are expressed as mean±standard deviation (SD) from three independent experiments, each performed with three technical replicates unless otherwise specified. For time-course CCK-8 assays, cell viability was analyzed using two-way analysis of variance (ANOVA) followed by Tukey's post hoc test for multiple comparisons. For single-time-point measurements, among-group differences were assessed by one-way ANOVA followed by Holm-Sidak's multiple-comparisons test. All statistical tests were two-tailed, with $P<0.05$ considered statistically significant. Analyses were performed using GraphPad Prism (version 9.0, GraphPad Software, San Diego, CA, USA).

RESULTS

SLC31A1 Knockdown Had Little Impact Under High Glucose Alone but Protected Against HG+Cu-Induced Loss of Viability and ATP To assess whether SLC31A1 knockdown modifies HG- and Cu-induced injury, we first analyzed CCK-8 time courses and ATP levels. Two-way ANOVA of CCK-8 signals showed significant effects of time, treatment, and their interaction (all $P<0.001$). Up to 24h, viability was similar across groups. From 48h onward, HG

alone modestly decreased viability versus NG, and comparable reductions were observed in HG+siCtrl and HG+siSLC31A1. HG+Cu+siCtrl caused the greatest loss of viability, whereas SLC31A1 knockdown significantly attenuated this decrease, with higher CCK-8 absorbance in HG+Cu+siSLC31A1 than in HG+Cu+siCtrl at 48–96h, although values remained below NG (Figure 1A). Consistently, ATP levels differed significantly among groups (one-way ANOVA, $P<0.001$; Figure 1B). HG, HG+siCtrl, and HG+siSLC31A1 showed reduced ATP versus NG, with no differences among the three HG groups. HG+Cu+siCtrl exhibited the most pronounced ATP depletion, whereas ATP in HG+Cu+siSLC31A1 was partially preserved, remaining higher than in HG+Cu+siCtrl but still lower than in NG, indicating that SLC31A1 knockdown mainly protects cellular energy status under Cu overload rather than under HG alone.

High Glucose and Cu Exacerbated Oxidative Stress, and SLC31A1 Knockdown Partially Normalizes Redox Indices Under Cu Overload To determine how HG, Cu, and SLC31A1 knockdown affect redox homeostasis, we measured GSH/GSSG, MDA, total SOD, CAT, and ROS. One-way ANOVA revealed significant between-group differences for all indices (all $P<0.001$; Figure 2). Compared with NG, HG increased oxidative stress, as indicated by lower GSH/GSSG and SOD/CAT activities and higher MDA and ROS. In the absence of Cu, these changes were similar among HG, HG+siCtrl, and HG+siSLC31A1, suggesting minimal basal effect of SLC31A1 knockdown under HG alone. Cu addition on top of HG further aggravated oxidative injury in HG+Cu+siCtrl, with additional decreases in GSH/GSSG and SOD/CAT and further elevation of MDA and ROS. SLC31A1 knockdown partially reversed these changes under Cu overload, as HG+Cu+siSLC31A1 showed higher GSH/GSSG and SOD/CAT and lower MDA and ROS than HG+Cu+siCtrl, but none of the indices returned to NG levels, indicating incomplete correction of Cu-aggravated oxidative stress.

SLC31A1-Dependent Cu Influx Drives Cu Overload and DLAT Lipoylation, with Limited Transcriptional Remodeling of the FDX1/LIAS/DLAT Axis To clarify whether SLC31A1 mediates Cu accumulation and cuproptosis signaling, we examined intracellular Cu, cuproptosis-related transcripts, and lipo-DLAT. Intracellular Cu content differed significantly among groups ($P<0.001$; Figure 3A). Cu levels were similar in all non-Cu-treated groups, whereas HG+Cu+siCtrl exhibited marked Cu overload that was significantly blunted by SLC31A1 knockdown in HG+Cu+siSLC31A1. SLC31A1, lipoic acid synthetase (LIAS), ferredoxin 1 (FDX1), and DLAT mRNA levels all showed significant between-group variation (all $P<0.001$; Figure 3B–3E). Under HG+Cu, SLC31A1 and FDX1 were upregulated, while LIAS and DLAT were downregulated; SLC31A1 knockdown partially reversed this pattern, increasing LIAS/DLAT and reducing FDX1 relative to HG+Cu+siCtrl. At the protein level, Cu superimposed on HG robustly increased SLC31A1 expression and the lipo-DLAT/total DLAT ratio, whereas siSLC31A1 markedly, but not completely, attenuated both (Figure 3F–3G). These findings indicate that SLC31A1-dependent Cu influx is a major driver of Cu overload and DLAT lipoylation, whereas downstream transcriptional modulation of the FDX1/LIAS/DLAT axis is only partial.

High Glucose and Cu Disrupted Tight Junction Gene Expression and Barrier Integrity, Which was Partially Rescued by SLC31A1 Knockdown To evaluate whether SLC31A1-dependent Cu toxicity affects endothelial barrier function, we assessed tight junction mRNAs, FITC-dextran permeability, and TEER. Zonula occludens-1 (ZO-1), Occludin, Claudin-5, FITC–dextran flux, and TEER were all significantly altered among groups (overall ANOVA, all $P<0.001$; Figure 4). HG alone modestly downregulated tight junction transcripts and caused mild increases in permeability and decreases in TEER versus NG, with no differences between HG, HG+siCtrl, and HG+siSLC31A1, indicating little basal effect of SLC31A1 knockdown in the absence of Cu. In contrast, HG+Cu+siCtrl produced the most severe barrier disruption, with pronounced repression of tight junction mRNAs, maximal FITC–dextran leakage, and the lowest TEER. SLC31A1 knockdown significantly improved both molecular and functional barrier indices under HG+Cu, partially restoring ZO-1, Occludin, and Claudin-5 expression, reducing FITC–dextran flux, and increasing TEER compared with HG+Cu+siCtrl, although barrier integrity remained inferior to NG, indicating partial but incomplete protection of endothelial junctions and barrier function during Cu overload.

DISCUSSION

Metal dyshomeostasis in retinal vascular disease may amplify ROS production, exacerbate oxidative and inflammatory injury, and ultimately compromise blood-retinal barrier integrity, whereas metal chelation may confer vasculoprotective effects[14]. Although DR has traditionally been regarded as a hyperglycemia-driven microvascular complication, accumulating evidence suggests that disturbances in trace metal homeostasis, particularly Cu, also contribute to retinal injury[6,15]. Bioinformatic and animal studies have identified the Cu importer SLC31A1 as a cuproptosis-related hub, upregulated in DR retinas, enriched in microglia, and associated with immune cell infiltration and cuproptotic remodeling[7]. In the present study, using HRMECs exposed to high glucose with or without Cu overload, we found that SLC31A1-dependent Cu influx was a major contributor to ATP depletion, oxidative stress, and endothelial barrier disruption

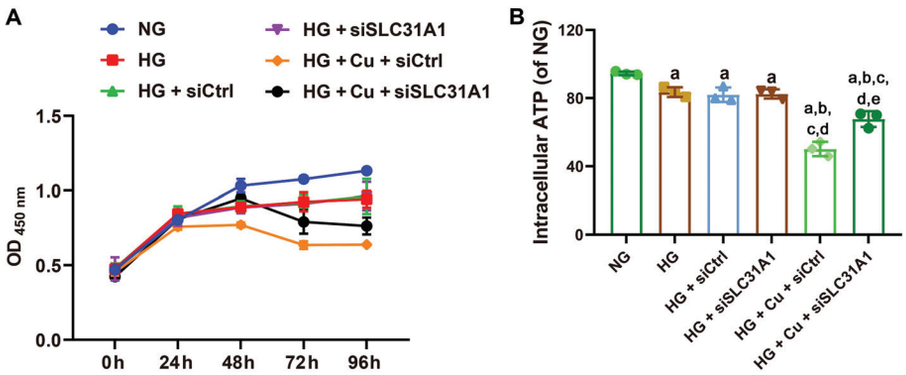

Figure 1 Effects of SLC31A1 knockdown, high glucose, and Cu on HRMEC viability and ATP levels A: Time course of cell viability in HRMECs cultured under NG, HG, HG+siCtrl, HG+siSLC31A1, HG+Cu+siCtrl, and HG+Cu+siSLC31A1 for 0, 24, 48, 72, and 96h, as assessed by the CCK-8 assay; B: Intracellular ATP content in the same six groups, measured using an ATP assay kit. Data are presented as mean±SD from three independent experiments. Statistical significance was assessed by two-way ANOVA with Tukey's post hoc test for panel A and one-way ANOVA with Holm-Sidak's post hoc test for panel B. [a]*P*<0.05 *vs* NG; [b]*P*<0.05 *vs* HG; [c]*P*<0.05 *vs* HG+siCtrl; [d]*P*<0.05 *vs* HG+siSLC31A1; [e]*P*<0.05 *vs* HG+Cu+siCtrl. NG: Normal glucose; HG: High glucose; Cu: Copper; siCtrl: Control small interfering RNA; siSLC31A1: SLC31A1 small interfering RNA; HRMECs: Human retinal microvascular endothelial cells; ATP: Adenosine triphosphate; CCK-8: Cell counting kit-8; SD: Standard deviation; ANOVA: Analysis of variance; OD: Optical density.

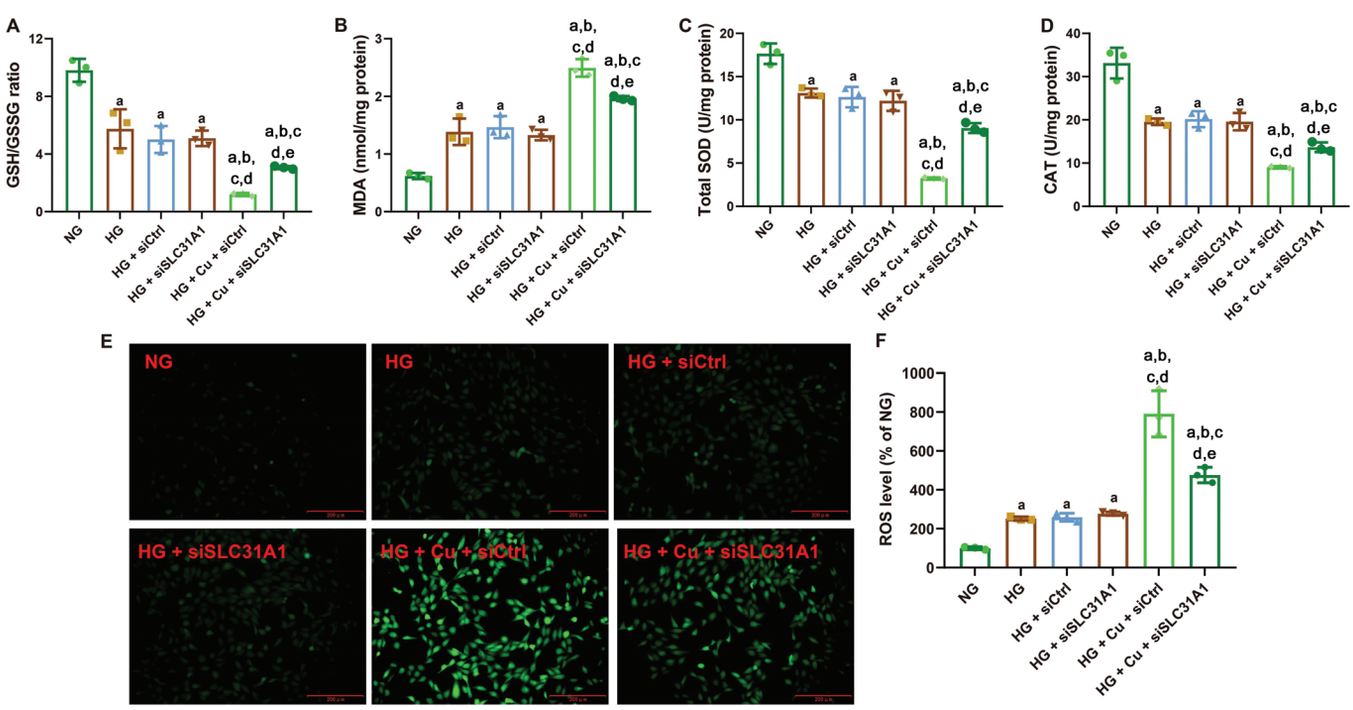

Figure 2 Effects of high glucose, Cu, and SLC31A1 knockdown on oxidative stress indices in HRMECs A: GSH/GSSG ratio; B: MDA levels; C: Total SOD activity; D: CAT activity, each measured using commercial biochemical assay kits; E–F: Intracellular ROS measured by DCFH-DA fluorescence. Data are presented as mean±SD from three independent experiments and were analyzed by one-way ANOVA with Holm-Sidak's post hoc test. [a]*P*<0.05 *vs* NG, [b]*P*<0.05 *vs* HG, [c]*P*<0.05 *vs* HG+siCtrl, [d]*P*<0.05 *vs* HG+siSLC31A1, [e]*P*<0.05 *vs* HG+Cu+siCtrl. NG: Normal glucose; HG: High glucose; Cu: Copper; siCtrl: Control small interfering RNA; siSLC31A1: SLC31A1 small interfering RNA; HRMECs: Human retinal microvascular endothelial cells; GSH/GSSG: Glutathione/oxidized glutathione; MDA: Malondialdehyde; SOD: Superoxide dismutase; CAT: Catalase; ROS: Reactive oxygen species; DCFH-DA: 2',7'-dichlorodihydrofluorescein diacetate; SD: Standard deviation; ANOVA: Analysis of variance.

under a diabetic-like milieu, whereas SLC31A1 knockdown conferred partial but consistent protection. Together with the observed increase in DLAT lipoylation, these findings support the involvement of cuproptosis-like signaling, although they do not constitute definitive evidence of canonical cuproptosis.

We selected 50 μmol/L $CuSO_4$ as a literature-informed acute Cu-overload challenge. Prior endothelial-cell studies showed

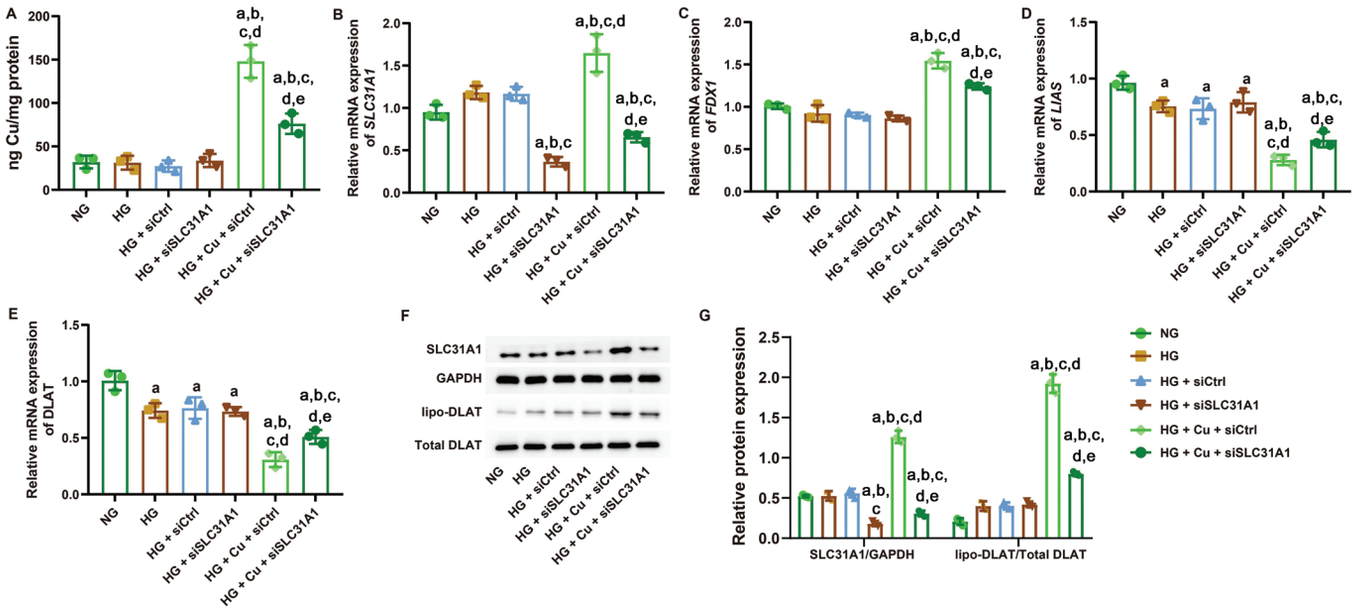

Figure 3 SLC31A1-dependent Cu influx, cuproptosis-related gene expression, and DLAT lipoylation in HRMECs A: Intracellular Cu content in HRMECs, measured using a Cu quantification kit; B–E: Relative mRNA expression of *SLC31A1* (B), *FDX1* (C), *LIAS* (D), and *DLAT* (E), determined by quantitative real-time PCR and normalized to GAPDH; F: Representative Western blots of SLC31A1, total DLAT, lipoylated DLAT (lipo-DLAT), and GAPDH in HRMECs; G: Densitometric quantification of SLC31A1/GAPDH and lipo-DLAT/total DLAT ratios. Data are presented as mean±SD from three independent experiments and were analyzed by one-way ANOVA with Holm-Sidak's post hoc test. [a]*P*<0.05 *vs* NG, [b]*P*<0.05 *vs* HG, [c]*P*<0.05 *vs* HG+siCtrl, [d]*P*<0.05 *vs* HG+siSLC31A1; [e]*P*<0.05 *vs* HG+Cu+siCtrl. NG: Normal glucose; HG: High glucose; Cu: Copper; siCtrl: Control small interfering RNA; siSLC31A1: SLC31A1 small interfering RNA; HRMECs: Human retinal microvascular endothelial cells; DLAT: Dihydrolipoamide S-acetyltransferase; LIAS: Lipoic acid synthetase; FDX1: Ferredoxin 1; GAPDH: Glyceraldehyde-3-phosphate dehydrogenase; PCR: Polymerase chain reaction; SD: Standard deviation; ANOVA: Analysis of variance.

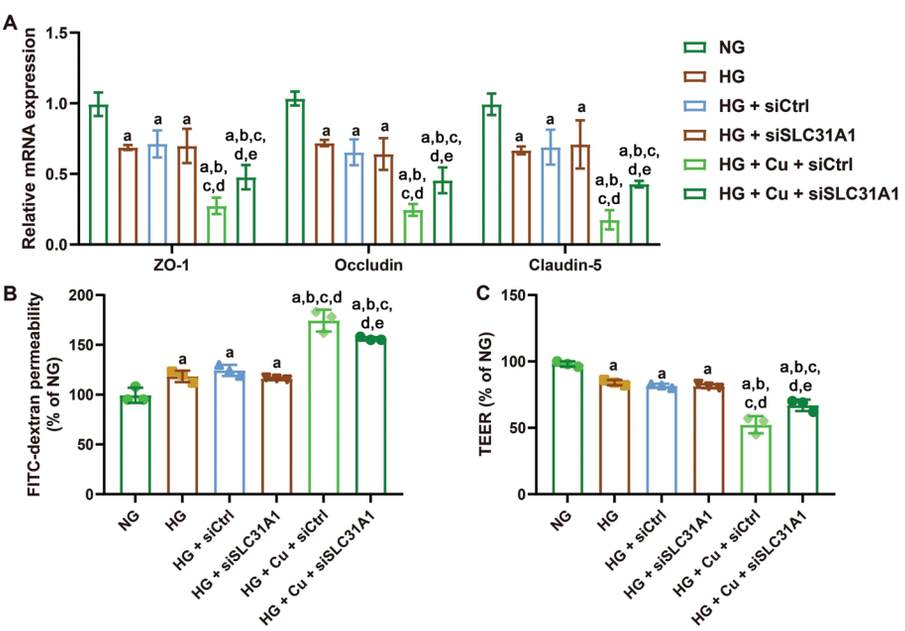

Figure 4 Effects of high glucose, Cu, and SLC31A1 knockdown on tight junction gene expression and barrier function in HRMECs A: Relative mRNA expression of the tight junction-related genes in HRMECs, assessed by quantitative real-time PCR and normalized to GAPDH; B: Paracellular permeability of HRMECs to 70-kDa FITC-dextran, measured using Transwell inserts; C: TEER of HRMEC monolayers cultured on Transwell inserts using an epithelial volt-ohmmeter. Data are presented as mean±SD from three independent experiments and were analyzed by one-way ANOVA with Holm-Sidak's post hoc test. [a]*P*<0.05 *vs* NG, [b]*P*<0.05 *vs* HG; [c]*P*<0.05 *vs* HG+siCtrl, [d]*P*<0.05 *vs* HG+siSLC31A1, [e]*P*<0.05 *vs* HG+Cu+siCtrl. NG: Normal glucose; HG: High glucose; Cu: Copper; siCtrl: Control small interfering RNA; siSLC31A1: SLC31A1 small interfering RNA; HRMECs: Human retinal microvascular endothelial cells; ZO-1: Zonula occludens-1; GAPDH: Glyceraldehyde-3-phosphate dehydrogenase; FITC-dextran: Fluorescein isothiocyanate-dextran; TEER: Transendothelial electrical resistance; PCR: Polymerase chain reaction; SD: Standard deviation; ANOVA: Analysis of variance.

that Cu in the 25–100 μmol/L range induced measurable endothelial responses without compromising short-term viability[12], and retinal-cell literature has also used high glucose combined with approximately 50 μmol/L Cu in ARPE-19 cells[13]. However, because a directly matching precedent in HRMECs has not been established, this condition should be interpreted as a literature-informed experimental setting rather than a definitively optimized HRMEC-specific paradigm. A key observation in our study was that SLC31A1 knockdown had little effect on the modest decline in viability and ATP induced by HG alone, but substantially attenuated the more severe ATP depletion and viability loss induced by HG+Cu. This pattern suggests that SLC31A1 is not a major determinant of basal mitochondrial dysfunction in hyperglycemia *per se*, but becomes more functionally relevant once extracellular Cu is increased. Cu is an essential cofactor for mitochondrial enzymes, yet excess Cu can catalyze Fenton-like reactions, damage Fe–S cluster proteins, and impair oxidative phosphorylation[16-17]. In an HG-stressed background, where mitochondrial respiration and redox balance are already compromised[18-19], additional Cu influx through SLC31A1 may therefore tip endothelial cells from compensated dysfunction into an energy crisis[20]. The ability of SLC31A1 knockdown to partially preserve ATP and viability under HG+Cu supports a model in which limiting Cu entry reduces mitochondrial burden and attenuates cuproptosis-like injury, although downstream damage is not completely normalized.

Oxidative stress is a central mechanism in DR pathogenesis, contributing to endothelial dysfunction, pericyte loss, and early blood-retinal barrier breakdown[21]. Across diverse organ systems, converging evidence places SLC31A1 at the intersection of Cu influx, oxidative stress, and cuproptosis-related injury. In intervertebral disc degeneration, oxidative stress upregulated specificity protein 1-driven SLC31A1 expression and Cu influx, enhancing FDX1-dependent tricarboxylic-acid cycle protein lipoylation and aggregation[22]. In cisplatin-induced acute kidney injury (AKI), E74-like ETS transcription factor 3 (ELF3)-mediated transcriptional activation of SLC31A1 drives excessive Cu entry, mitochondrial dysfunction, oxidative stress, and cuproptosis-related injury[23]. In sepsis-associated AKI, SLC31A1 upregulation similarly promoted Cu overload, oxidative/inflammatory injury, whereas reduced glutathione ameliorates injury partly by lowering Cu levels and suppressing SLC31A1 expression[24]. Our findings in HRMECs are consistent with this broader mechanistic framework. HG alone modestly decreased the reduced GSH/GSSG ratio and antioxidant enzyme activities and increased MDA and ROS, in keeping with classical hyperglycemia-induced oxidative stress[25]. These effects were similar among HG, HG+siCtrl, and HG+siSLC31A1, suggesting that SLC31A1 knockdown does not materially alter basal redox status in the absence of Cu overload. By contrast, adding Cu on top of HG markedly aggravated oxidative injury, whereas SLC31A1 silencing partially reversed these changes. Mechanistically, this is plausible because excess Cu, as a redox-active transition metal, can fuel ROS generation and propagate oxidative damage, particularly in mitochondria. Thus, by limiting Cu influx, SLC31A1 knockdown likely reduces the intracellular Cu pool available for redox cycling and attenuates oxidative injury in an already HG-stressed environment. These findings support SLC31A1 as an important amplifier of oxidative stress in HRMECs under Cu-overload conditions and link Cu dyshomeostasis to the oxidative component of DR.

We further explored how SLC31A1-mediated Cu entry may interface with the canonical cuproptosis machinery. In the established model, FDX1 acts upstream to reduce Cu^{2+} to Cu^{+} and promote lipoylation of TCA cycle enzymes such as DLAT, whereas LIAS supplies the lipoic acid cofactor; when Cu is excessive, Cu-bound lipoylated DLAT contributes to aggregation of lipoylated mitochondrial proteins and loss of Fe–S cluster proteins, culminating in cuproptotic cell death[26-28]. In our system, neither HG nor SLC31A1 knockdown alone altered basal intracellular Cu levels, whereas HG+Cu induced marked Cu overload that was significantly blunted by SLC31A1 silencing. At the transcriptional level, Cu supplementation under HG upregulated SLC31A1 and FDX1 and further suppressed LIAS and DLAT, whereas SLC31A1 knockdown partially reversed these changes. At the protein level, Cu robustly increased SLC31A1 expression and markedly enhanced DLAT lipoylation, both of which were attenuated, although not completely normalized, by SLC31A1 knockdown. Together with the relatively modest transcriptional remodeling of FDX1 and LIAS, these data suggest that SLC31A1-mediated Cu influx primarily amplifies cuproptosis-related signaling rather than definitively establishing a complete canonical cuproptosis program.

Importantly, SLC31A1 should not be viewed in isolation. Cu homeostasis is regulated by a broader trafficking network that includes ATP7A and ATP7B, which govern Cu efflux and intracellular redistribution[5]. Accordingly, the incomplete rescue observed after SLC31A1 silencing may reflect residual Cu trafficking through complementary transport systems as well as the contribution of parallel stress pathways. In addition, SLC31A1 has been linked to VEGFR2 signaling[10], and DR-related studies have associated it with inflammatory remodeling and immune-cell infiltration[7]. These links suggest that Cu dyshomeostasis may aggravate endothelial dysfunction not only through mitochondrial injury and redox imbalance but also through angiogenic and inflammatory signaling pathways

relevant to DR progression. Thus, the present findings support the concept that SLC31A1 participates in a broader Cu-handling and stress-response network that may interact with oxidative, inflammatory, and angiogenic mechanisms in the diabetic retina.

Endothelial barrier integrity is a clinically relevant readout in DR[29]. In Alzheimer's disease, upregulated SLC31A1 and impaired Cu export lead to hippocampal Cu accumulation; *in vitro*, amyloid-beta 42-induced ROS accumulation, TEER loss, and cadherin 5 phosphorylation in human brain microvascular endothelial cells are reversed by Cu chelation or CTR1/SLC31A1 knockdown, highlighting Cu-transport-dependent oxidative barrier dysfunction[30]. In our HRMEC model, HG alone caused modest downregulation of tight junction genes, slightly increased FITC-dextran permeability, and reduced TEER, consistent with mild inner barrier impairment typical of early DR. These HG-induced changes were not influenced by SLC31A1 knockdown, matching its limited effect on oxidative stress and ATP under HG alone. In contrast, HG+Cu induced pronounced barrier disruption, with marked suppression of tight junction transcripts, maximal paracellular leakage, and the lowest TEER. Under these conditions, SLC31A1 knockdown significantly improved both molecular and functional barrier indices, although barrier integrity remained inferior to that of normal glucose conditions. These data indicate that SLC31A1-dependent Cu handling is not only a metabolic stressor but also contributes to endothelial barrier failure in a diabetic-like environment.

This study has several limitations. First, all experiments were conducted in an HRMEC monoculture system *in vitro*. Although HRMECs are widely used to investigate retinal endothelial dysfunction in DR, this model cannot fully recapitulate the chronic and multicellular retinal microenvironment *in vivo*, where endothelial cells dynamically interact with pericytes, Müller cells, microglia, neurons, extracellular matrix components, and hemodynamic influences. Therefore, the present findings should be interpreted primarily as evidence for an endothelial cell-autonomous role of SLC31A1 under high-glucose plus Cu exposure, rather than as a complete representation of the *in vivo* disease process. Second, an osmotic control group was not included. Although prior retinal endothelial-cell studies commonly used matched mannitol controls and often reported minimal effects on selected endpoints[31-32], we cannot completely exclude a contribution of hyperosmolar stress, particularly for redox-related readouts, in our experimental system. Third, the Cu treatment condition used in this study was selected on the basis of prior endothelial-cell literature rather than systematic optimization in HRMECs. Fourth, we relied solely on siRNA-mediated SLC31A1 knockdown without complementary gain-of-function approaches or pharmacological interventions, and we did not test Cu chelators or other rescue strategies; such studies would strengthen causal inference and translational relevance. Fifth, although the observed changes in DLAT lipoylation, ATP depletion, and oxidative stress were consistent with cuproptosis involvement, we did not rigorously distinguish cuproptosis from other regulated cell death pathways, such as apoptosis, ferroptosis, or necroptosis. Finally, morphological assessment of HRMEC injury was limited. Although the biochemical, molecular, and functional data consistently supported cellular injury under high-glucose plus Cu exposure, direct visual evidence of morphological alterations was lacking. Future studies incorporating imaging-based morphological analyses, multicellular retinal models, and *in vivo* validation will be important to further define the role of SLC31A1-mediated Cu dysregulation in DR.

SLC31A1 plays a context-dependent role in HRMECs: it has little impact on the modest dysfunction induced by HG alone but becomes an important mediator of Cu-aggravated injury, such that SLC31A1 knockdown significantly attenuates Cu-driven ATP loss, oxidative damage, intracellular Cu accumulation, DLAT hyper-lipoylation, and tight junction disruption while partially preserving endothelial barrier integrity. These findings support SLC31A1-mediated Cu influx as a mechanistic link between diabetic metabolic stress, cuproptosis-like mitochondrial injury, and blood-retinal barrier breakdown, and suggest that SLC31A1 may be a potential therapeutic target for protecting the retinal microvasculature in DR.

ACKNOWLEDGEMENTS

Authors' Contributions: Li Y and Chen M designed and performed the experiments, collected and analyzed the data, prepared the figures, and drafted the manuscript; Dong HG Chen M conceived and supervised the study, contributed to study design and data interpretation, and critically revised the manuscript for important intellectual content. All authors read and approved the final manuscript.

Conflicts of Interest: Li Y, None; **Chen M,** None; **Dong HG,** None.

REFERENCES

1 Seo H, Park SJ, Song M. Diabetic retinopathy (DR): mechanisms, current therapies, and emerging strategies. *Cells* 2025;14(5):376.

2 Teo ZL, Tham YC, Yu M, *et al*. Global prevalence of diabetic retinopathy and projection of burden through 2045. *Ophthalmology* 2021;128(11):1580-1591.

3 GBD 2019 Blindness and Vision Impairment Collaborators; Vision Loss Expert Group of the Global Burden of Disease Study. Causes of blindness and vision impairment in 2020 and trends over 30 years, and prevalence of avoidable blindness in relation to VISION 2020: the Right to Sight: an analysis for the Global Burden of Disease Study. *Lancet Glob Health* 2021;9(2):e144-e160.

4 Koksaldi S, Karti O, Saatci AO. Anti-vascular endothelial growth factor therapies in ophthalmology. *Med Hypothesis Discov Innov Ophthalmol* 2025;14(3):107-135.

5 Lutsenko S, Roy S, Tsvetkov P. Mammalian copper homeostasis: physiological roles and molecular mechanisms. *Physiol Rev* 2025;105(1):441-491.

6 Chang WG, Li PF. Copper and diabetes: current research and prospect. *Mol Nutr Food Res* 2023;67(23):2300468.

7 Hu Q, Zhang X, Huang JY, *et al*. The STAT1-SLC31A1 axis: Potential regulation of cuproptosis in diabetic retinopathy. *Gene* 2024;930:148861.

8.Wang C, Wu JH, Wang Y, *et al*. The role of dysregulated copper metabolism in diabetes and its complications: a review. *Front Endocrinol (Lausanne)* 2025;16:1681001.

9 El-Nablaway M, Sonpol HMA, Ali Elewa YHA, *et al*. Copper chelation by penicillamine protects against doxorubicin-induced cardiomyopathy by suppressing FDX1-mediated cuproptosis. *Biomolecules* 2025;15(9):1320.

10 Das A, Ash D, Fouda AY, *et al*. Cysteine oxidation of copper transporter CTR1 drives VEGFR2 signalling and angiogenesis. *Nat Cell Biol* 2022;24(1):35-50.

11 Chen ZG, Liu WM, *et al*. Inhibition of viability of human retinal microvascular endothelial cells by vialinin A under high glucose condition. *Int J Ophthalmol* 2024;17(10):1809-1815.

12 Wei H, Zhang WJ, LeBoeuf R, *et al*. Copper induces–and copper chelation by tetrathiomolybdate inhibits–endothelial activation *in vitro*. *Redox Rep* 2014;19(1):40-48.

13 Dhivya MA, Sulochana KN, Bharathi Devi SR. High glucose induced inflammation is inhibited by copper chelation *via* rescuing mitochondrial fusion protein 2 in retinal pigment epithelial cells. *Cell Signal* 2022;92:110244.

14 Li Y, Luo T, *et al*. Therapeutic potential of iron chelators in retinal vascular diseases. *Int J Ophthalmol* 2023;16(11):1899-1910.

15 Yang J, Gao YC, Mao H, *et al*. Qiju Dihuang Pill protects the lens epithelial cells *via* alleviating cuproptosis in diabetic cataract. *J Ethnopharmacol* 2024;333:118444.

16 Genchi G, Catalano A, Carocci A, *et al*. Copper, cuproptosis, and neurodegenerative diseases. *Int J Mol Sci* 2025;26(18):9173.

17 Xiao SZ, Liu TC, Li N, *et al*. Chloride-mediated enhancement in Cu(II)-catalyzed Fenton-like reaction: The overlooked reactive chlorine species. *Environ Pollut* 2024;360:124586.

18 Dassanayaka S, Readnower RD, Salabei JK, *et al*. High glucose induces mitochondrial dysfunction independently of protein O-GlcNAcylation. *Biochem J* 2015;467(1):115-126.

19 Bhatt NM, Aon MA, Tocchetti CG, *et al*. Restoring redox balance enhances contractility in heart trabeculae from type 2 diabetic rats exposed to high glucose. *Am J Physiol Heart Circ Physiol* 2015;308(4):H291-H302.

20 Prasad Panda S, Kesharwani A. Micronutrients/miRs/ATP networking in mitochondria: Clinical intervention with ferroptosis, cuproptosis, and calcium burden. *Mitochondrion* 2023;71:1-16.

21 Gao J, Tao LM, Jiang ZX. Alleviate oxidative stress in diabetic retinopathy: antioxidant therapeutic strategies. *Redox Rep* 2023;28:2272386.

22 Chen X, Li K, Xiao Y, *et al*. SP1/CTR1-mediated oxidative stress-induced cuproptosis in intervertebral disc degeneration. *Biofactors* 2024;50(5):1009-1023.

23 Qiu ZM, Liu QC, Wang L, *et al*. The copper transporter, SLC31A1, transcriptionally activated by ELF3, imbalances copper homeostasis to exacerbate cisplatin-induced acute kidney injury through mitochondrial dysfunction. *Chem Biol Interact* 2024;393:110943.

24 Wang L, Jiang L, Wang JJ, *et al*. Reduced glutathione ameliorates sepsis-induced acute kidney injury in mouse model: involvement of cuproptosis. *Ren Fail* 2025;47:2518227.

25 Singh A, Kukreti R, Saso L, *et al*. Mechanistic insight into oxidative stress-triggered signaling pathways and type 2 diabetes. *Molecules* 2022;27(3):950.

26 Liu WQ, Lin WR, Yan L, *et al*. Copper homeostasis and cuproptosis in cancer immunity and therapy. *Immunol Rev* 2024;321(1):211-227.

27 Li HJ, Li YC, Yu YH, *et al*. GSH exhaustion *via* inhibition of xCT-GSH-GPX4 pathway synergistically enhanced DSF/Cu-induced cuproptosis in myelodysplastic syndromes. *Free Radic Biol Med* 2024;222:130-148.

28 Song XH, Ding YH, Chen JS. Tumor glucose reprogramming suppresses cuproptosis: a review. *Biomol Biomed* 2025;26(2):251-261.

29 Darwish NHE, Hussein KA, Elmasry K, *et al*. Bone morphogenetic protein-4 impairs retinal endothelial cell barrier, a potential role in diabetic retinopathy. *Cells* 2023;12(9):1279.

30 Hossain MS, Das A, Rafiq AM, *et al*. Altered copper transport in oxidative stress-dependent brain endothelial barrier dysfunction associated with Alzheimer's disease. *Vasc Pharmacol* 2024;157:107433.

31 El-Remessy AB, Abou-Mohamed G, Caldwell RW, *et al*. High glucose-induced tyrosine nitration in endothelial cells: role of eNOS uncoupling and aldose reductase activation. *Invest Ophthalmol Vis Sci* 2003;44(7):3135-3143.

32 Zeng Y, Cui ZK, Liu J, *et al*. MicroRNA-29b-3p promotes human retinal microvascular endothelial cell apoptosis *via* blocking SIRT1 in diabetic retinopathy. *Front Physiol* 2020;10:1621.